

QUT Digital Repository:
<http://eprints.qut.edu.au/>



This is the author version published as:

Frost, Ray L. and Cheng, Hongfei and Yang, Jing (2010)
*Thermogravimetric analysis of selected coal-bearing strata
kaolinite*. *Thermochimica Acta*, 507/8. pp. 84-90.

Copyright 2010 Elsevier BV

Thermogravimetric analysis of selected coal-bearing strata kaolinite

Hongfei Cheng ^{a,b,c}, Qinfu Liu ^a, Jing Yang ^c, Ray L. Frost ^{c*}

^a School of Geoscience and Surveying Engineering, China University of Mining and Technology, Beijing 100083, China

^b School of Mining Engineering, Inner Mongolia University of Science and Technology, Baotou 014010, china

^c School of Physical and Chemical Sciences, Queensland University of Technology, 2 George Street, GPO Box 2434, Brisbane, Queensland 4001, Australia

Abstract: Two kinds of coal-bearing kaolinite from China were analysed by X-ray diffraction (XRD), Thermogravimetric analysis-mass spectrometry (TG-MS), infrared emission spectroscopy. Thermal decomposition occurs in a series of steps attributed to (a) desorption of water at 68 °C for Datong coal bearing strata kaolinite and 56 °C for Xiaoxian with mass losses of 0.36 % and 0.51 % (b) decarbonization at 456 °C for Datong coal bearing strata kaolinite and 431 °C for Xiaoxian kaolinite, (c) dehydroxylation takes place in two steps at 589 and 633 °C for Datong coal bearing strata kaolinite and at 507 °C and 579 °C for Xiaoxian kaolinite. This mineral were further characterised by infrared emission spectroscopy (IES). Well defined hydroxyl stretching bands at around 3695, 3679, 3652 and 3625 cm⁻¹ are observed. At 650 °C all intensity in these bands is lost in harmony with the thermal analysis results. Characteristic functional groups from coal are observed at 1918, 1724 and 1459 cm⁻¹. The intensity of these bands decrease by thermal treatment and is lost by 700 °C.

Key words: Thermal analysis; thermogravimetry, Coal-bearing; Kaolinite; infrared emission spectroscopy

* Author to whom correspondence should be addressed (r.frost@qut.edu.au)

1 **1. Introduction**

2 Kaolinite-rich mineral deposits are very abundant in the Permo-Carboniferous
3 coal-bearing strata of North China and are widely used [1]. It was found that kaolinite
4 usually existed in the upper part of sedimentary cycle, deposited vertically, which was
5 formed in the hydrodynamic environment from strong to weak [2]. Some deposits
6 have high carbon content and form hard minerals. Almost all coal measures of
7 Northern China contain the industrial kaolinite rocks which generally contain a
8 significant amount of organic compounds. The color of coal-bearing kaolinite is rather
9 dark, varying from light gray to gray black to almost completely black [1-3]. In recent
10 years, different researchers have put forward a number of classification programs for
11 the coal-measures kaolinite minerals. The further study of coal-measures kaolinite
12 bearing minerals, based on different factors, such as the material sources, creation
13 environment, late reformation, and industrial value. It is concluded that the
14 sedimentary alteration of volcanic ash may be the main formation mode of kaolinite
15 coal bearing minerals, but not the only one [3].

16
17 The thermal transformation of kaolinite has been investigated by Brown et al.
18 1985 [4, 5], He et al. 1995 [6] and others [7-12]. The coal bearing kaolinite rocks are
19 often finely ground and calcined at 950 °C. At this temperature kaolinite is
20 transformed to metakaolinite. It is generally agreed that kaolinite forms metakaolinite
21 by heating in the temperature range 550 °C to 950 °C and mullite mainly forms at
22 temperatures above 1150 °C. Mullite is an important constituent in refractories,
23 whitewares and structural clay products when kaolinite is frequently used as the raw
24 material [13]. Therefore, the calcination of coal bearing kaolinite minerals has been
25 used to prepare mullite.

26
27 The calcined kaolin is often used in the rubber and plastic, ceramic raw material,
28 fiberglass, cracking catalysts, cosmetics, medicines and other polymers [14-17].
29 Properties of calcined kaolin, particularly important for industrial applications, are

30 thermal stability and whiteness [16, 18]. Thus, this study of the thermal stability of
31 coal bearing strata kaolinite rocks is of great important in calcined kaolin industrial
32 applications. The thermal analysis of coal bearing strata kaolinite also gives new
33 insights not only about improvement of the properties but also serves to protect the
34 environment.

35

36 In current study, to the best of the authors' knowledge no thermoanalytical
37 studies of the thermal stability of coal bearing kaolinite have been undertaken;
38 although differential thermal analysis of some related minerals has been published
39 [19-23]. This paper reports the thermal analysis of two coal bearing strata kaolinite
40 using XRD, TG-MS and infrared emission spectroscopy.

41

42 **2. Experimental methods**

43 **2.1 Materials**

44 The raw materials used in this work are tonstein, which are kaolinite claystone of
45 volcanic origin found as partings in coal seams of Permo-Carboniferous strata in
46 Datong (Kd) coal mines from Shanxi province in North China and
47 Permo-Carboniferous strata in Xiaoxian (Kx) from Anhui province in China (Table 1).
48 The beds of Datong coal bearing kaolinite are about 0.5 m thick and are widespread in
49 the coal-bearing strata of the Datong coalfield. The kaolinite content in the rocks is up
50 to 95 % and the quality is very good for industrial use.

51

52 **2.2 X-ray diffraction**

53 X-ray diffraction patterns were collected using a PANalytical X'Pert PRO X-ray
54 diffractometer (radius: 240.0 mm). Incident X-ray radiation was produced from a line
55 focused PW3373/10 Cu X-ray tube, operating at 40 kV and 40 mA, with Cu K α
56 radiation of 1.540596 Å. The incident beam passed through a 0.04 rad soller slit, a
57 1/2 ° divergence slit, a 15 mm fixed mask, and a 1 ° fixed antiscatter slit.

58

59 **2.3 Thermogravimetric analysis and mass spectrometric**

60 Thermogravimetric analysis (TG) of the samples was carried out in a TA[®]
61 Instruments incorporated high-resolution thermo gravimetric analyser (series Q500) in
62 a flowing nitrogen atmosphere ($60 \text{ cm}^3 \text{ min}^{-1}$). Approximately 50 mg of each sample
63 underwent thermal analysis, with a heating rate of $5 \text{ }^\circ\text{C}/\text{min}$, with resolution of 6,
64 from $25 \text{ }^\circ\text{C}$ to $1000 \text{ }^\circ\text{C}$. The TG instrument was coupled to a Balzers (Pfeiffer) mass
65 spectrometer for gas analysis. Only water vapour, carbon dioxide, and oxygen were
66 analysed using mass spectrometry.

67

68 **2.4 Infrared emission spectroscopy**

69 FTIR emission spectroscopy was carried out on a Nicolet Nexus 870 FTIR
70 spectrometer, which was modified by replacing the IR source with an emission cell. A
71 description of the cell and principles of the emission experiment have been published
72 elsewhere [24-28]. Approximately 0.2 mg of coal bearing strata kaolinite was spread
73 as a thin layer on a 6mm diameter platinum surface and held in an inert atmosphere
74 within a nitrogen-purged cell during heating. The infrared emission cell consists of a
75 modified atomic absorption graphite rod furnace, which is driven by a
76 thyristor-controlled AC power supply capable of delivering up to 150 A at 12 V. A
77 platinum disk acts as a hot plate to heat the coal bearing strata kaolinite sample and is
78 placed on the graphite rod. An insulated $125 \text{ }\mu\text{m}$ type R thermocouple was embedded
79 inside the platinum plate in such a way that the thermocouple junction was less than
80 0.2 mm below the surface of the platinum. Temperature control of $\pm 2 \text{ }^\circ\text{C}$ at the
81 operating temperature of the sample was achieved by using a Eurotherm Model 808
82 proportional temperature controller, coupled to the thermocouple.

83

84 In the normal course of events, three sets of spectra are obtained over the
85 temperature range selected and at the same temperatures; those of the black body
86 radiation, the platinum plate radiation, and the platinum plate covered with the sample.
87 Normally only one set of black body and platinum radiation is required. The emission

88 spectrum at a particular temperature was calculated by subtraction of the single beam
89 spectrum of the platinum backplate from that of the platinum covered with the sample,
90 and the result ratioed to the single beam spectrum of an approximate black body
91 (graphite). This spectral manipulation is carried out after all the spectral data has been
92 collected.

93

94 The emission spectra were collected at intervals of 50 °C over the range
95 100-1000 °C. The time between scans (while the temperature was raised to the next
96 hold point) was approximately 100 s. It was considered that this was sufficient time
97 for the heating block and the powdered sample to reach temperature equilibrium. The
98 spectra were acquired by co-addition of 128 scans for the whole temperature range,
99 with an approximate scanning time of 1 min, and a nominal resolution of 4 cm⁻¹.
100 Good quality spectra can be obtained providing the sample thickness is not too large.
101 If too large a sample is used then the spectra become difficult to interpret due to the
102 presence of combination and overtone bands. Spectral manipulation such as baseline
103 adjustment, smoothing and normalization was performed using the Spectra calc
104 software package (Galactic Industries Corporation, NH, USA).

105

106 **3. Results and discussion**

107 **3.1 X-ray diffraction (XRD) and chemical composition**

108 The XRD patterns of the two coal-bearing strata kaolinites together with standard
109 XRD patterns are shown in Fig. 1. The XRD patterns of the kaolinites show identical
110 patterns to the standards. The XRD patterns of these two kaolinite minerals show an
111 impurity of quartz. The degree of structural disorder of the coal bearing strata
112 kaolinite samples can be evaluated on the basis of the XRD background in the range
113 $2\theta=20-30^\circ$, and the width of the (002) diffraction peak $d=0.358$ nm at half the
114 maximum height [29-32]. The intensity of coal bearing kaolinite in the $d(022)$,
115 $d(1\bar{3}0)$, $d(\bar{1}31)$, $d(003)$, $d(1\bar{3}1)$ and $d(\bar{1}13)$ peak suggest that the kaolinite is low
116 defect kaolinite. Structural order in these samples was estimated using the Hinckley

117 index (HI) [30]. The samples from two different area clearly revealed an increase in
118 the ordering in the sense $K_x=1.03 < K_d=1.35$.

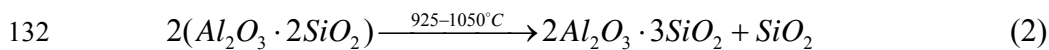
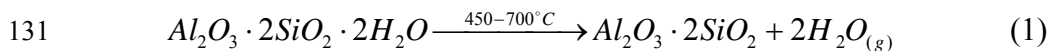
119

120 The chemical composition of the two coal bearing strata kaolinite is reported in
121 Table 2. The result shows the two coal bearing strata kaolinite including more SiO_2
122 than general kaolinite about 45 %, especially in Xiaoxian kaolinite rock.

123

124 3.2 Thermogravimetric analysis and mass spectrometric analysis

125 Kaolinite is a hydrous layer silicate clay mineral. The structural unit of kaolinite
126 consists of a Si-O tetrahedral sheet and an Al-O(OH) octahedral sheet [33]. Kaolinite
127 is transformed to metakaolinite as the structural water is driven off at temperatures
128 from 550–950 °C [1]. It is reported that two main thermal induced processes take
129 place for kaolinite. The whole process can be mostly described by the reaction [13,
130 34-40]:

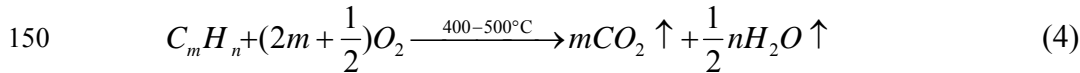


133 The phase transformations are expressed in the form of chemical reactions for
134 the ease of explanation. However, the above equations are unable describe the coal
135 bearing strata kaolinite exactly. It is influenced by the degree of disorder of the
136 kaolinite structure, formation environment and the amount and kind of impurities [8,
137 34, 41-43].

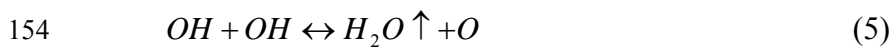
138 The thermogravimetric and differential thermogravimetric analysis of coal
139 bearing strata kaolinite are shown in Fig. 2. The associated mass spectrometric
140 analysis is reported in Fig. 3. The first small mass loss is observed at 68 °C for Kd and
141 56 °C for Kx and the mass loss is 0.36 % and 0.51 %. These two mass loss steps are
142 attributed to desorption of adsorbed water.

143 A second mass loss step is observed at 456 °C for Datong coal bearing strata
144 kaolinite and 431 °C for Xiaoxian, which was indicated by MS to be the release of
145 CO_2 from coal (Fig.2 and 3). Yang et al. proposed a set of steps for the dehydration

146 and hydrocarbon of coal and organic from coal bearing strata kaolinite [44]. These
147 steps correspond to (a) the loss of carbon (b) the loss of organic. Such a scheme is
148 represented by the following chemical equation:



151 When coal bearing strata kaolinite lose their so-called “structural water”, OH
152 radicals in the structure react together to form water, and the process may be
153 represented by an equation of the type [7, 38]



155 It is obvious that the mainly dehydration reaction has three stages. The mass loss
156 step is observed at 526 °C for Kd and 463 °C for Kx with mass loss of 3.54 and
157 3.76 %, which is attributed to the decomposition of hydrocarbon from coal. The
158 another mass loss steps occur around 589 °C for Kd and 507 °C for Kx with a mass
159 loss of 4.3 % and 3.03 %. These mass loss steps are assigned to the dehydroxylation
160 of inner surface OH units. The last mass loss of 3.56 % at 633 °C for Kd and 3.71 %
161 at 579 °C for Kx are observed, which are attributed to the water release from the
162 octahedral coordinated Al^{3+} ion could generate isolated OH groups or inner hydroxyl
163 units [38, 45]. Heating the coal bearing strata kaolinite results in a loss of hydroxyls.
164 Subsequent exposure to the air results in water being adsorbed and a layer of
165 hydroxyls formed on the surface of metakaolinite [1].

166

167 The mass spectrometric gas-release studies can be used to study simultaneously
168 the composition of evolved gases during the thermal treatment [38]. It is well known
169 that the chemical composition of kaolinite is $Al_2Si_2O_5(OH)_4$. In accordance with
170 former findings no distinct stage of dehydration has occurred (at about 450 °C).
171 However, this are unable describe the decomposition of coal bearing strata kaolinite
172 exactly. Because most of coal bearing strata kaolinite in China contains a certain
173 amount of organic. In order to clarify the decomposition mechanism of coal bearing
174 strata kaolinite, the mass loss during each decomposition process should be

175 characterized by the identified evolution components.

176 The ion current curves for the evolved gases show for $m/Z=18$ and $m/Z=17$ a
177 mass gain at 68 °C for Kd and 56 °C for Kx (Figure 3a and b). A further mass gain of
178 water vapour occurs at around 589 °C for Kd and 507 °C for Kx. At these two
179 temperatures OH units are lost from the coal bearing kaolinite structure. Another ion
180 current curves for the evolved gases show for $m/Z=44$ a mass gain at 456 °C for Kd
181 and 431 °C for Kx, which is attributed to the burning of coal present in coal bearing
182 strata kaolinite. A further mass gain of CO_2 occurs at about 720 °C, which is assigned
183 to decomposition of little amount carbonate impurity. The mass gain in the MS curves
184 corresponds precisely with the mass loss in the TG curves.

185

186 **3.3 Infrared emission spectroscopy**

187 Typical infrared emission spectra of coal bearing strata kaolinite of Kd and Kx
188 are show in Fig.4. The spectra clearly show the temperature at which the OH groups
189 are lost; in the case of Kd the temperature is 700 °C and Kx is 650 °C. The bands of
190 some organic from coal appear to be lost before the temperature at 700 °C for Kd and
191 600 °C for Kx. In the 500-700 °C temperature for Kd and 400-600 °C for Kx range a
192 broad spectral feature is observed. In order to follow these thermal decomposition
193 three spectra at 300, 500 and 700 °C were selected for further analysis.

194

195 The infrared emission spectra of Kd and Kx in the $3550-3750\text{ cm}^{-1}$ region at 300,
196 500 and 700 °C are shown in Fig. 5a and b, respectively. The higher wavenumber
197 bands at $(\nu_1)3695$, $(\nu_2)3679$, $(\nu_3)3652$ and $(\nu_5)3625\text{ cm}^{-1}$ for Kd and $(\nu_1)3695$,
198 $(\nu_2)3675$, $(\nu_3)3654$ and $(\nu_5)3625\text{ cm}^{-1}$ for Kx are attributed to the hydroxyl stretching
199 of the inner surface hydroxyl, out-of-phase vibration of the inner surface hydroxyls,
200 the second out-of-phase vibration of the inner surface hydroxyls and inner hydroxyls
201 [12, 46-48]. In the 300 °C, the spectrum bands ν_1 , ν_2 , ν_3 and ν_5 are observed. The
202 500 °C spectrum of Kd shows a small shift in these bands, which are now observed at
203 3705, 3673, 3652 and 3625 cm^{-1} and the band ν_1 disappeared for Kx. In the 700 °C

204 spectrum, the four bonds all disappeared.

205

206 The infrared emission spectra at 300, 500 and 700 °C for Kd and Kx in the
207 1400-2000 cm^{-1} range are shown in Figs. 6a and b, respectively. The band separation
208 occurs for coal bearing strata kaolinite in this spectral region. The band at 1456 cm^{-1}
209 in the 300 °C for Kd and 1459 cm^{-1} for Kx is attributed to the C=C stretching
210 vibrations, whereas the band at 1710 cm^{-1} for Kd and 1724 cm^{-1} for Kx is assigned to
211 the C=O or COOH stretching vibrations. The band is observed at 1822 cm^{-1} t in the
212 300 °C for Kd and 1820 cm^{-1} for Kx are attributed to the C-O stretching vibrations. An
213 additional band at 1911 cm^{-1} in the 300 °C for Kd and 1918 cm^{-1} for Kx is observed
214 which is attributed to the C=O vibration [49, 50]. These bands are observed for Kd
215 and Kx at 300 °C; at 500 °C the band at 1911, 1710 and 1456 cm^{-1} for Kd and 1915,
216 1720 cm^{-1} for Kx; and at 700 °C only the band at 1970 cm^{-1} .

217

218 **4. Conclusions**

219 The thermal decomposition of two coal bearing strata kaolinite have been
220 analysed and studied. The temperatures of dehydroxylation and decarbonization found
221 in the coal bearing kaolinites have been achieved using TG-MS and infrared emission
222 spectroscopy, a very useful technique for determining the thermal decomposition and
223 stability of these minerals. TG-MS and infrared emission spectra show the coal
224 bearing kaolinite released CO_2 about 450 °C. Thus for protection environment
225 decarbonization before calcination coal bearing strata kaolinite is necessary.

226

227

228

229 **Acknowledgment**

230 The authors gratefully acknowledge the financial support provided by the National
231 “863” project of China (2008AA06Z109) and infra-structure support of the

- 232 Queensland University of Technology Inorganic Materials Research Program of the
233 School of Physical and Chemical Science.

References

- [1] Q.F. Liu, D.A. Spears, Q.P. Liu, *Applied Clay Science* 19 (2001) 89-94.
- [2] S.L. Ding, Q.F. Liu, Y.Z. Sun, B.H. Xu, *World Journal of Engineering* 6 (2009) 1-6.
- [3] S.L. Ding, Q.F. Liu, M.Z. Wang, *Procedia Earth and Planetary Science* 1 (2009) 1024-1028.
- [4] K.J.D. MacKenzie, I.W.M. Brown, R.H. Meinhold, M.E. Bowden, *Journal of the American Ceramic Society* 68 (1985) 293-297.
- [5] I.W.M. Brown, K.J.D. Mackenzie, M.E. Bowden, R.H. Meinhold, *Journal of the American Ceramic Society* 68 (1985) 298-301.
- [6] H. He, C. Hu, J. Guo, H. Zhang, *Chinese Journal of Geochemistry* 14 (1995) 78-82.
- [7] G.W. Brindley, M. Nakahira, *Journal of the American Ceramic Society* 40 (1957) 346-350.
- [8] J.G. Cabrera, M. Eddleston, *Thermochimica Acta* 70 (1983) 237-247.
- [9] A. Gaylord D, G. Paul D, *Journal of the American Ceramic Society* 57 (1974) 132-135.
- [10] J.B. Howard, K. Frank, *Journal of the American Ceramic Society* 52 (1969) 199-203.
- [11] J.S. Killingley, S.J. Day, *Fuel* 69 (1990) 1145-1149.
- [12] R.L. Frost, *Clays And Clay Minerals* 46 (1998) 280-289.
- [13] C.Y. Chen, G.S. Lan, W.H. Tuan, *Ceramics International* 26 (2000) 715-720.
- [14] F. Franco, L.A. Pérez-Maqueda, J.L. Pérez-Rodríguez, *Journal Of Colloid And Interface Science* 274 (2004) 107-117.
- [15] X. Zhang, D. Fan, Z. Xu, *Journal of Tongji University (Natural Science)* 33 (2005) 1646-1650.
- [16] F. Franco, J.A. Cecilia, L.A. Pérez-Maqueda, J.L. Pérez-Rodríguez, C.S.F. Gomes, *Applied Clay Science* 35 (2007) 119-127.
- [17] E. Mako, J. Kristof, E. Horvath, V. Vagvolgyi, *Journal Of Colloid And Interface Science* 330 (2009) 367-373.
- [18] H.H. Murray, I. Wilson, *Applied Clay Mineralogy. Occurrences, Processing and Application of Kaolins, Bentonite, Palygorskite-Sepiolite, and Common Clays*, 2007.
- [19] D. Galusek, Z. Lences, P. Sajgalik, R. Riedel, *Journal of Mining and Metallurgy, Section B: Metallurgy* 44 (2008) 35-38.
- [20] G. Meng, Z. Xu, X. Qi, W. Yang, Z. Xie, *Gongye Cuihua* 15 (2007) 1-5.
- [21] A. Leszczynska, K. Pielichowski, *Journal of Thermal Analysis and Calorimetry* 93 (2008) 677-687.
- [22] A.J. Locke, W.N. Martens, R.L. Frost, *Thermochimica Acta* 459 (2007) 64-72.
- [23] L.K. Joseph, H. Suja, G. Sanjay, S. Sugunan, V.P.N. Nampoore, P. Radhakrishnan, *Applied Clay Science* 42 (2009) 483-487.
- [24] R.L. Frost, S. Bahfenne, J. Graham, *Spectrochimica Acta Part A: Molecular and Biomolecular Spectroscopy* 71 (2008) 1610-1616.
- [25] R.L. Frost, G.A. Cash, J.T. Kloprogge, *Vibrational Spectroscopy* 16 (1998) 173-184.
- [26] R.L. Frost, J.T. Kloprogge, *Spectrochimica Acta Part A: Molecular and Biomolecular Spectroscopy* 55 (1999) 2195-2205.
- [27] R.L. Frost, M.L. Weier, *Thermochimica Acta* 406 (2003) 221-232.
- [28] R. Frost, D. Wain, *Journal of Thermal Analysis and Calorimetry* 91 (2008) 267-274.
- [29] G. Kakali, T. Perraki, S. Tsvilis, E. Badogiannis, *Applied Clay Science* 20 (2001) 73-80.

- [30] D.N. Hinckley, *Clays And Clay Minerals* 11 (1963) 229-235.
- [31] R. Vigil de la Villa, F. Moisés, S.d.R.M. Isabel, V. Iñigo, G. Rosario, *Applied Clay Science* 36 (2007) 279-286.
- [32] C. He, E. Makovicky, B. Osbaeck, *Applied Clay Science* 9 (1994) 165-187.
- [33] R.L. Frost, *Clay Minerals* 32 (1997) 65-77.
- [34] P. Ptacek, D. Kubatova, J. Havlica, J. Brandstetr, F. Soukal, T. Opravil, *Thermochimica Acta* In Press, Corrected Proof.
- [35] O. Castelein, B. Soulestin, J.P. Bonnet, P. Blanchart, *Ceramics International* 27 (2001) 517-522.
- [36] Y.-F. Chen, M.-C. Wang, M.-H. Hon, *Journal of the European Ceramic Society* 24 (2004) 2389-2397.
- [37] R.L. Frost, H. Erzsébet, M. Éva, K. János, R. Ákos, *Thermochimica Acta* 408 (2003) 103-113.
- [38] K. Heide, M. Foldvari, *Thermochimica Acta* 446 (2006) 106-112.
- [39] S.J. Chipera, D.L. Bish, *Clays and Clay Minerals* 50 (2002) 38-46.
- [40] V. Balek, M. Murat, *Thermochimica Acta* 282-283 (1996) 385-397.
- [41] M. Földvári, *Journal of Thermal Analysis and Calorimetry* 48 (1997) 107-119.
- [42] K. Nahdi, P. Llewellyn, F. Rouquerol, R. J., N.K. Ariguib, M.T. Ayedi, *Thermochimica Acta* 390 (2002) 123-132.
- [43] L. Heller-Kallai, *Journal of Thermal Analysis and Calorimetry* 50 (1997) 145-156.
- [44] X. Yang, S. Hu, X. Chen, P. Zhuo, F. Xiang, *Journal of China Coal Society* 33 (2008) 566-569.
- [45] L. Heller-Kallai, I. Miloslavski, A. Grayevsky, *American Mineralogist* 74 (1989) 818-820.
- [46] R.L. Frost, J. Kristof, E. Mako, E. Horvath, *Spectrochimica Acta Part A: Molecular and Biomolecular Spectroscopy* 59 (2003) 1183-1194.
- [47] R.L. Frost, J. Kristof, G.N. Paroz, J.T. Klopogge, *Journal of Colloid and Interface Science* 208 (1998) 216-225.
- [48] R.L. Frost, S.J. van der Gaast, *Clay Minerals* 32 (1997) 471-484.
- [49] X. Shu, W. Zuna, J. Xu, L. Ge, *Journal of Fuel Chemistry and Technology* 24 (1996) 426-433.
- [50] Z. Zhu, C. Han, C. Zhang, *Journal of Fuel Chemistry and Technology* 27 (1999) 335-339.

LIST OF TABLES

Table1 Kaolin samples

Table 2 the chemical composition of the coal bearing kaolinites

Table1 Kaolin samples

Kaolin Sample	Location	Content of Kaolinite	Particle Size	Impurities
Kaolinite(Kd)	Shanxi Datong, China	97%	-45 μ m	Quartz
Kaolinite(Kx)	Anhui Xiaoxian, China	93%	-45 μ m	Quartz

Table 2 the chemical composition of the coal bearing kaolinites

samples	SiO ₂	Al ₂ O ₃	TFe ₂ O ₃	MgO	CaO	Na ₂ O	K ₂ O	TiO ₂	P ₂ O ₅	MnO	LOT
Taiyuan	53.54	30.13	1.52	1.33	0.39	0.72	0.60	0.12	<0.1	0.065	11.61
Xiaoxian	62.36	27.54	0.88	0.63	0.05	0.11	0.64	0.04	<0.1	0.117	6.91

LIST OF FIGURES

Fig.1 the XRD patterns of coal bearing strata kaolinite (a)Kd and (b) Kx

Fig. 2 TGA-DTG curves of coal bearing kaolinite (a)Kd and (b) Kx

Fig. 3 Evolved gas analysis for coal bearing kaolinite (a)Kd and (b) Kx

Fig. 4 Infrared emission spectra of coal bearing kaolinite (a)Kd and (b)Kx over the 100- 1000°C

Fig.5 Infrared spectra of (a)Kd and (b)Kx in the 3550-3750cm⁻¹ region at 300, 500 and 700°C

Fig.6 Infrared spectra of (a)Kd and (b)Kx in the 1400-2000cm⁻¹ region at 300,500 and 700°C

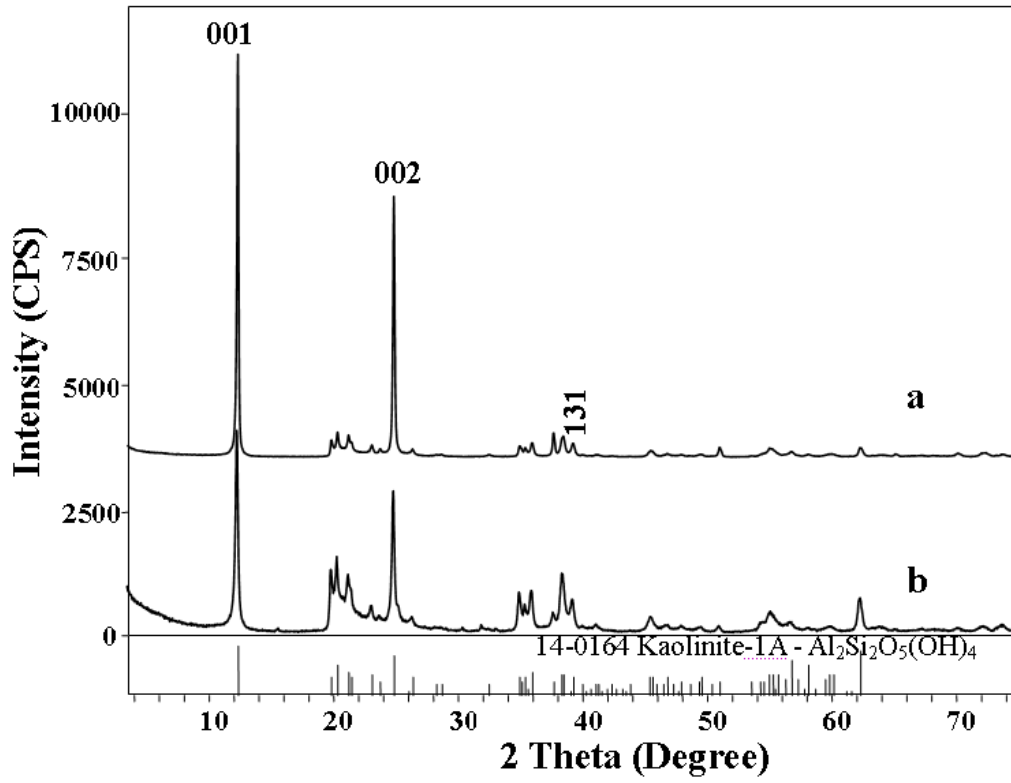
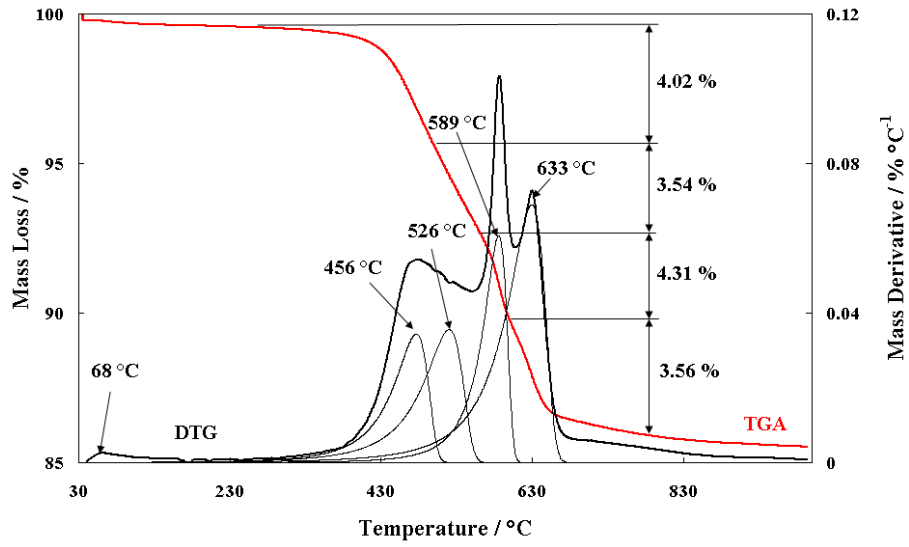
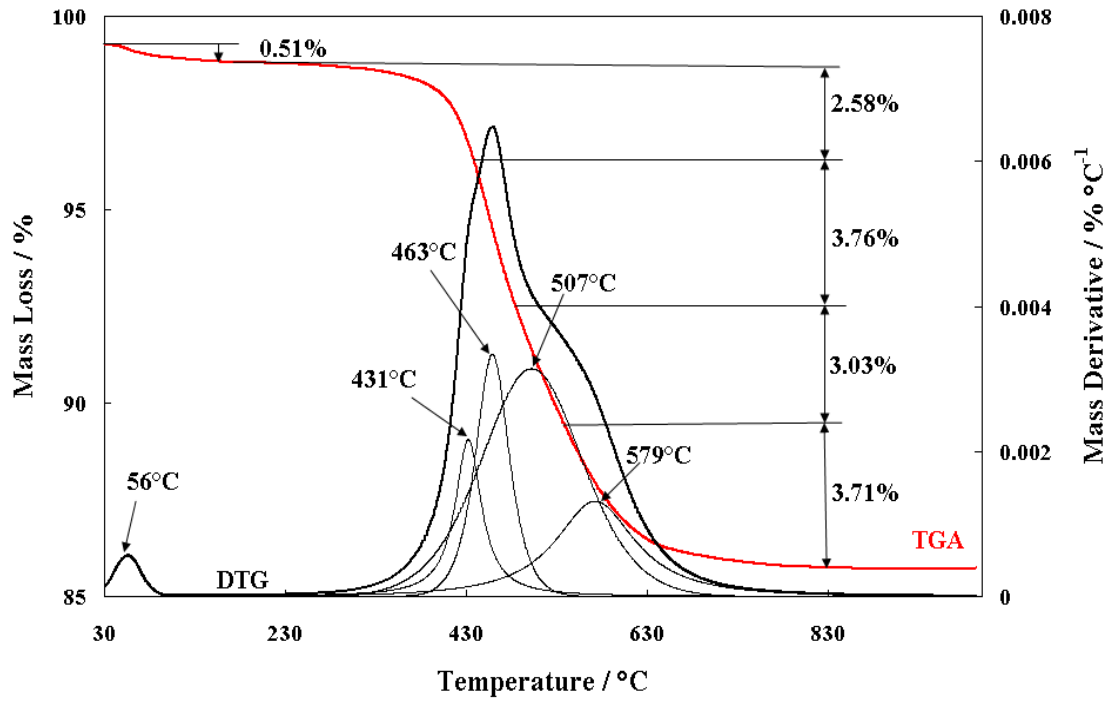


Fig.1 The XRD patterns of coal bearing strata kaolinite (a) Kd and (b) Kx

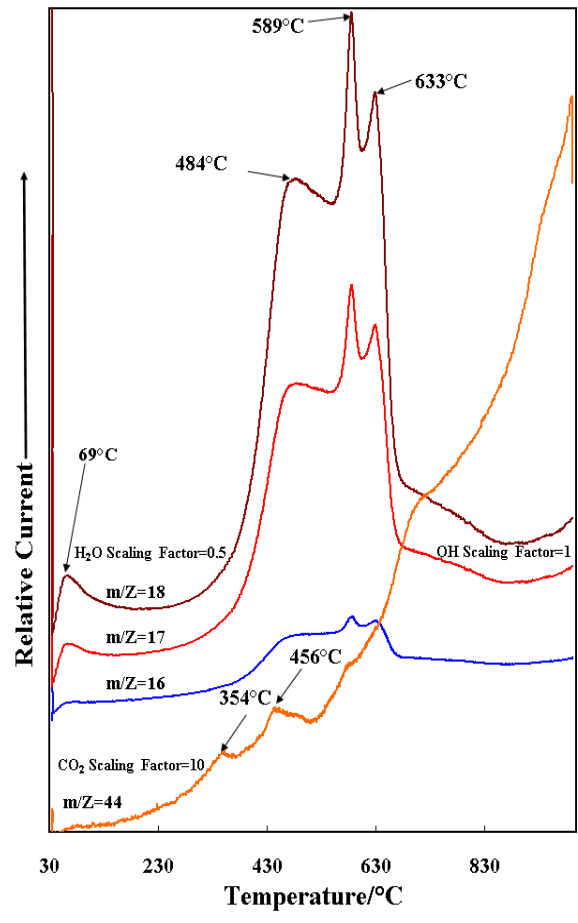


a

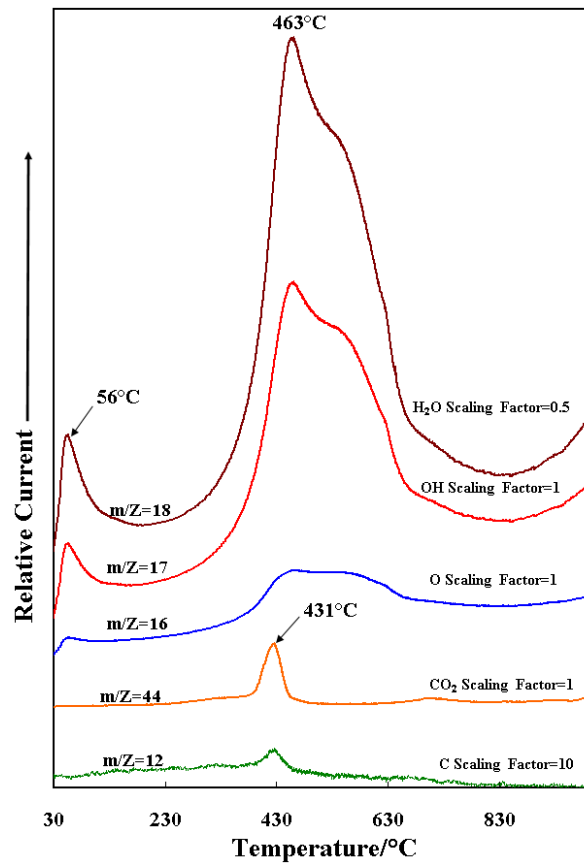


b

Fig. 2 TGA-DTG curves of coal bearing kaolinite (a) Kd and (b) Kx

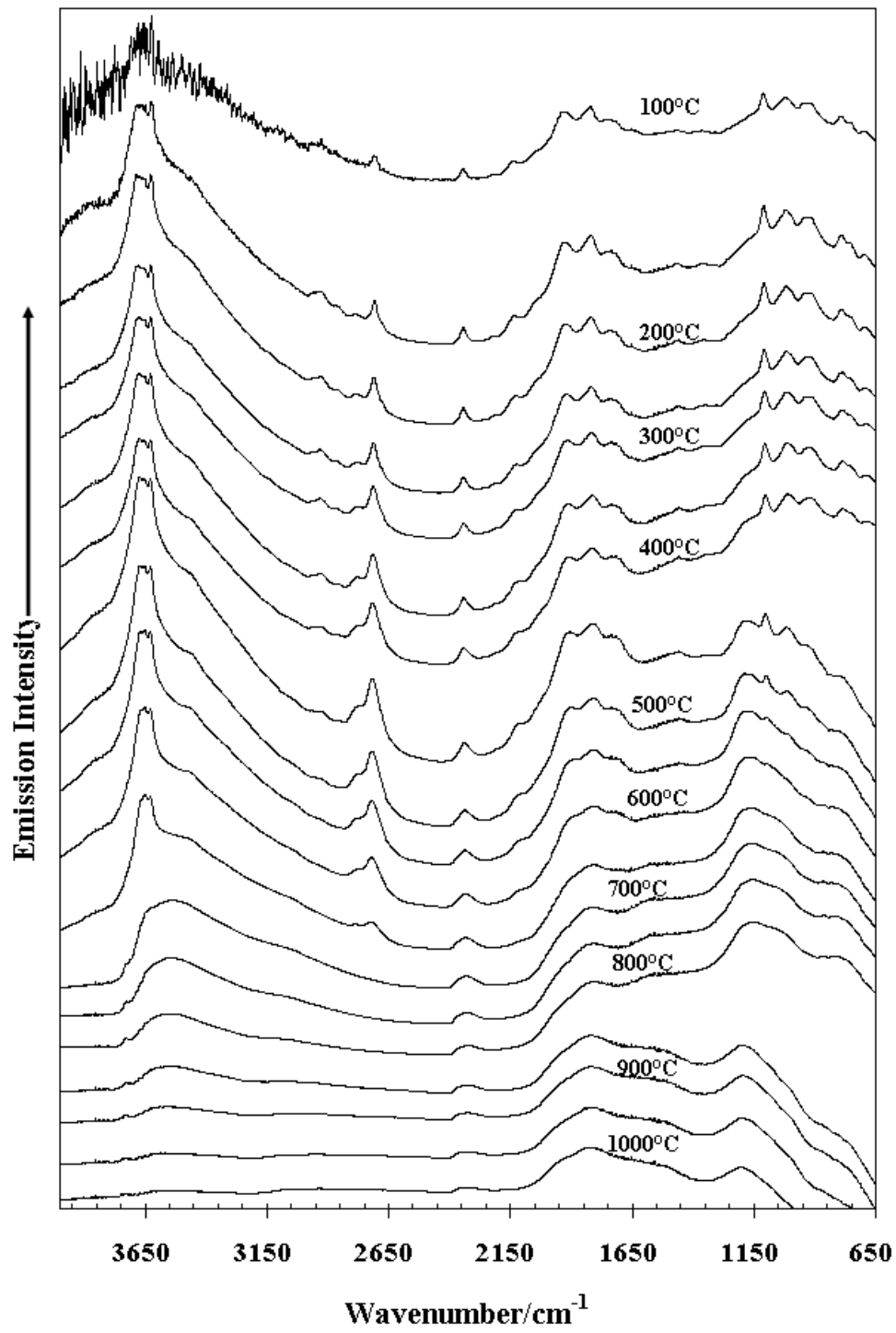


a

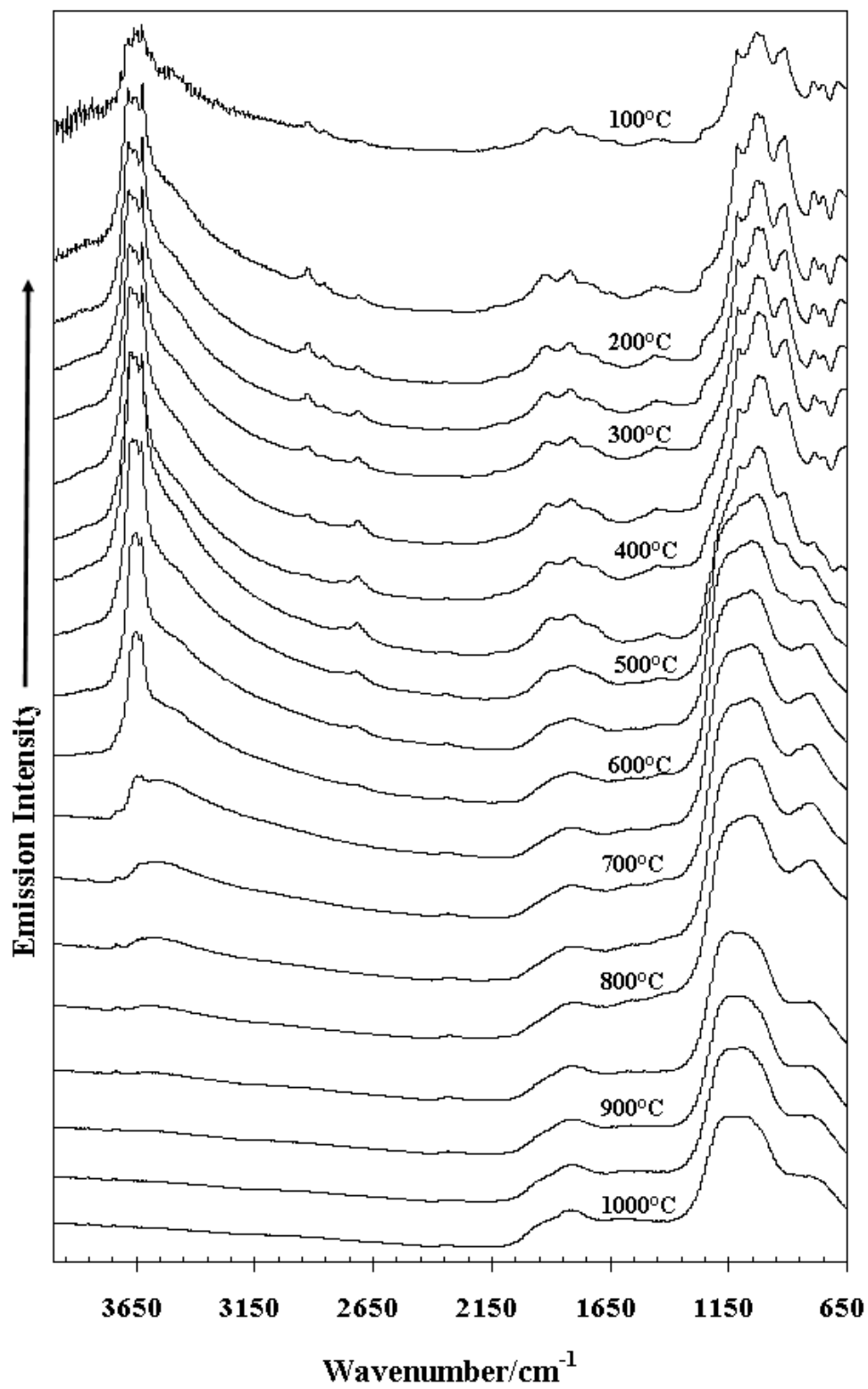


b

Fig. 3 Evolved gas analysis for coal bearing kaolinite (a) Kd and (b) Kx

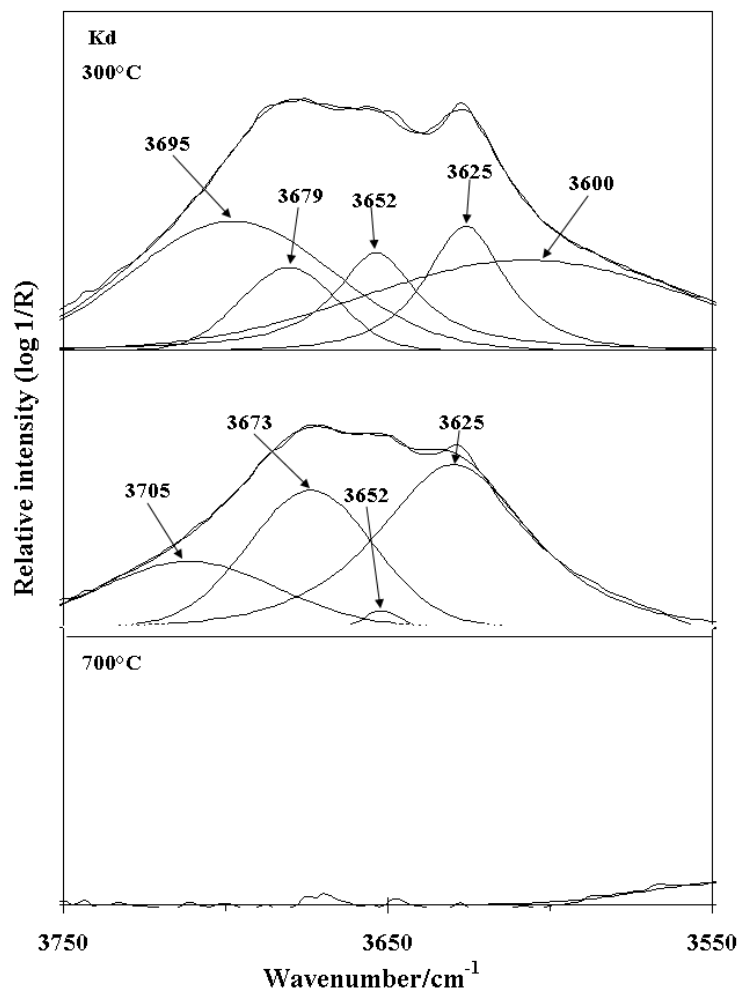


a

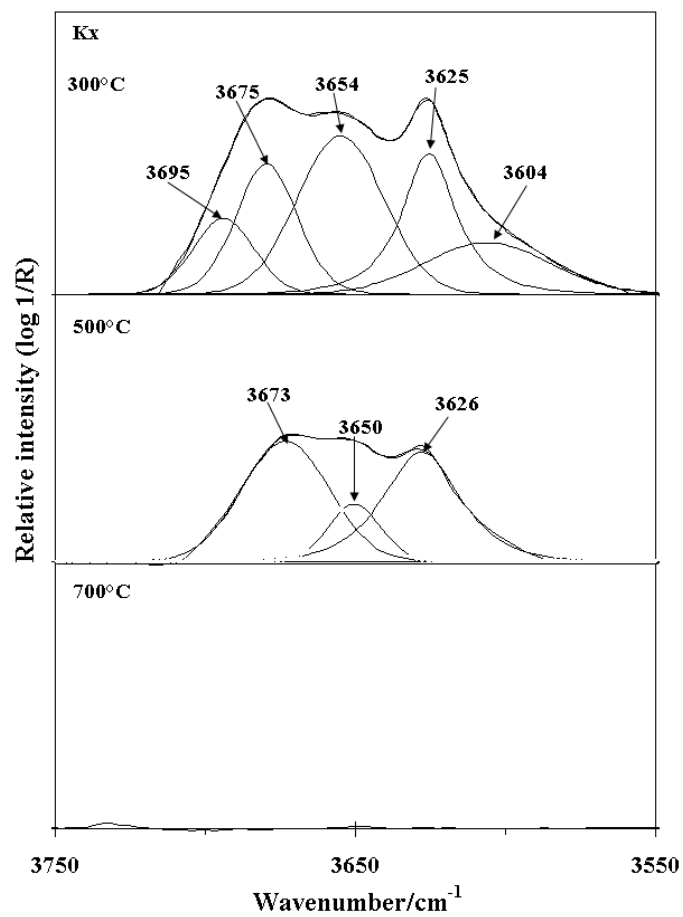


b

Fig. 4 Infrared emission spectra of coal bearing kaolinite (a)Kd and (b)Kx over the 100-1000°C

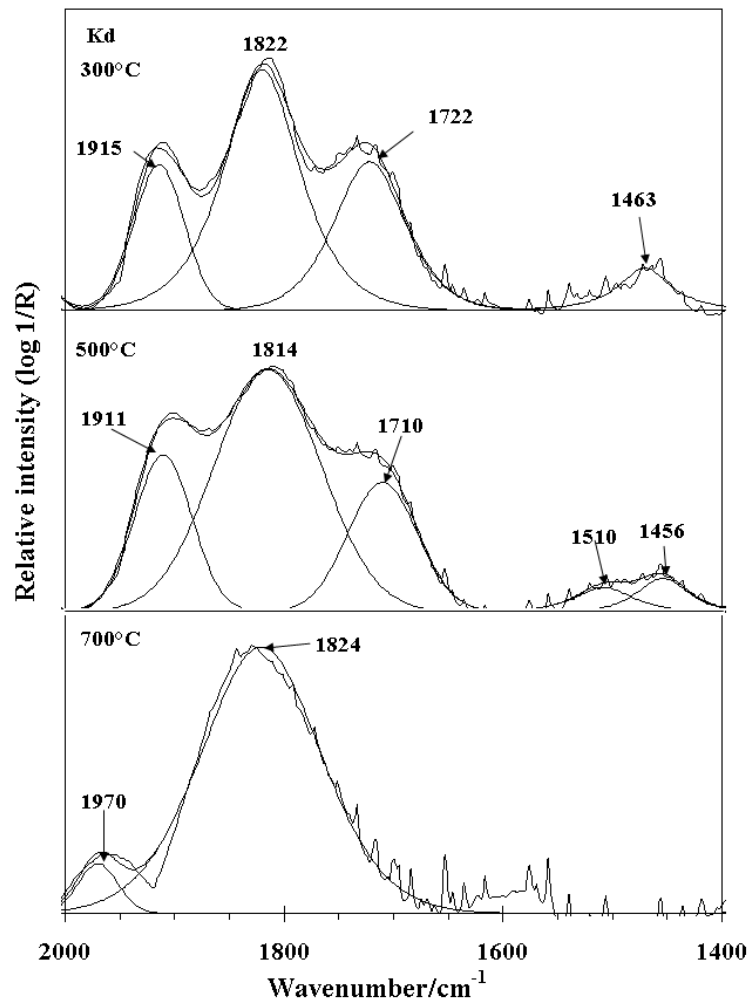


a

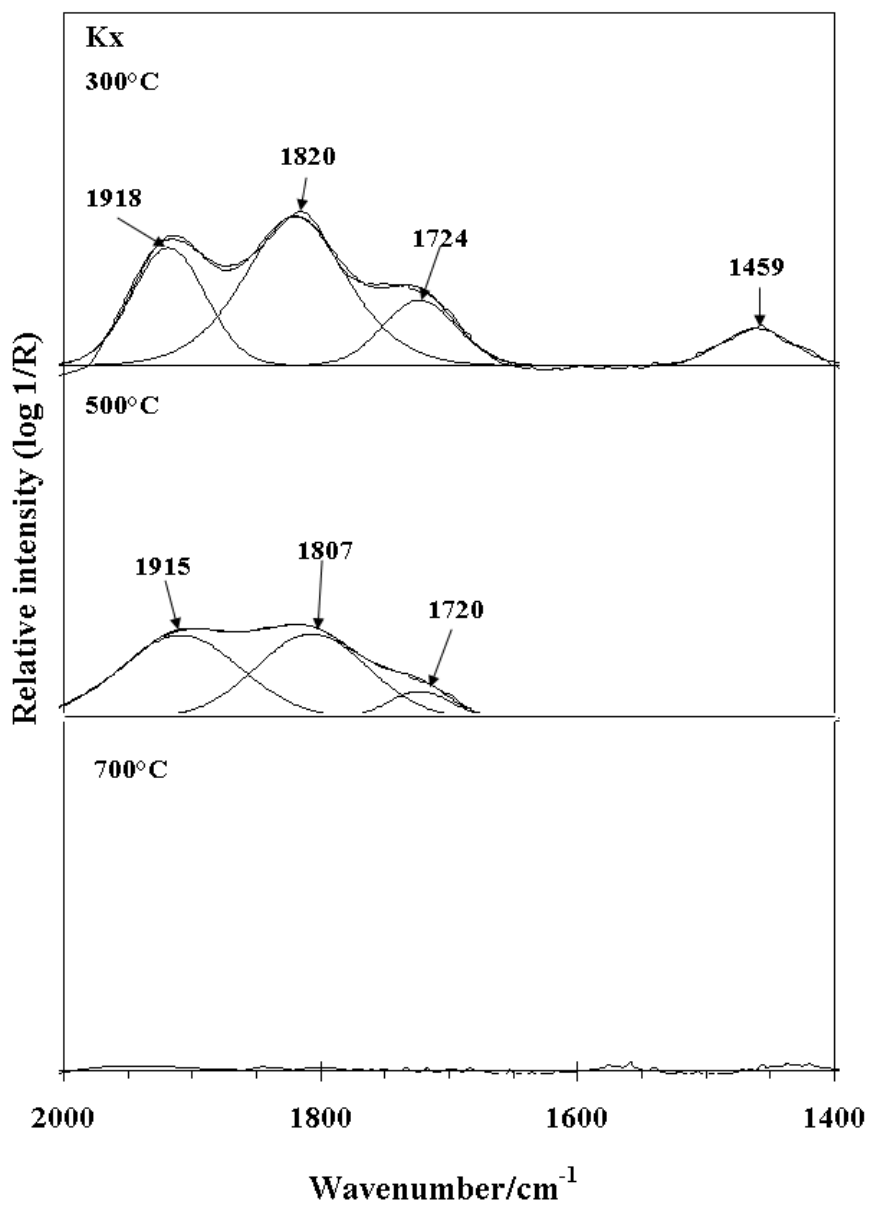


b

Fig.5 Infrared spectra of (a)Kd and (b)Kx in the $3550\text{-}3750\text{cm}^{-1}$ region at $300, 500$ and 700°C



a



b

Fig.6 Infrared spectra of (a) Kd and (b) Kx in the $1400\text{-}2000\text{cm}^{-1}$ region at 300,500 and 700°C